A Modeling Study of Circulation and Eddies in the Persian Gulf

PRASAD G. THOPPIL AND PATRICK J. HOGAN

Open Ocean Processes and Prediction Section, Naval Research Laboratory, Stennis Space Center, Mississippi

(Manuscript received 27 January 2009, in final form 12 April 2010)

ABSTRACT

The circulation and mesoscale eddies in the Persian Gulf are investigated using results from a high-resolution (~1 km) Hybrid Coordinate Ocean Model (HYCOM). The circulation in the Persian Gulf is composed of two spatial scales: basin scale and mesoscale. The progression of a cyclonic circulation cell dominates the basin-scale circulation in the eastern half of the gulf (52°–55°E) during March–July. This is primarily the consequence of density-driven outflow–inflow through the Strait of Hormuz and strong stratification. A northwestward-flowing Iranian Coastal Current (ICC; 30–40 cm s^{-1}) between the Strait of Hormuz and north of Qatar (~52°E) forms the northern flank of the cell. Between July and August the ICC becomes unstable because of the baroclinic instability mechanism by releasing the potential energy stored in the cross-shelf density gradient. As a result, the meanders in the ICC evolve into a series of mesoscale eddies, which is denoted as the Iranian coastal eddies (ICE). The ICE have a diameter of about 115–130 km and extend vertically over most of the water column. Three cyclonic eddies produced by the model during August–September 2005 compared quite well with the Moderate Resolution Imaging Spectroradiometer (MODIS) SST and chlorophyll-*a* observations. The remnants of ICE are seen until November, after which they dissipate as the winter cooling causes the thermocline to collapse.

1. Introduction

The Persian Gulf (also known as the Arabian Gulf) is a shallow, semienclosed basin with a mean depth of about 35 m and is connected to the Gulf of Oman through the Strait of Hormuz (Fig. 1). The circulation in the Persian Gulf is primarily driven by the prevailing northwesterly winds and the associated momentum and buoyancy fluxes, secondarily by thermohaline forcing, and thirdly by the tides. A typical basin-scale circulation of the gulf is cyclonic and composed of a northwestward-flowing Iranian Coastal Current (ICC) from the Strait of Hormuz along the northern side of the basin with speeds greater than 10 cm s^{-1} (Hunter 1983) and a southeastward-flowing current in the southern portion of the gulf (Fig. 34 of Reynolds 1993). The former, which flows against the prevailing northwesterly winds, is primarily driven by the pressure gradient (Chao et al. 1992; Lardner et al. 1993; Blain 2000). The tidal influence on the circulation in the Persian Gulf is insignificant, except in the Strait of Hormuz and along the Iranian coast (Blain 1998).

Circulation and water mass formation in the Persian Gulf have been the subject of several previous modeling studies (Lardner et al. 1987, 1988, 1989, 1993; Lardner and Das 1991; Chao et al. 1992; Horton et al. 1992; Song et al. 1994; Blain 2000; Azam et al. 2006; Elshorbagy et al. 2006; Kämpf and Sadrinasab 2006). Several of these studies used either hydrodynamic numerical models or spectral models of coarse to moderate horizontal resolutions (20–5 km) and were driven by density only or monthly atmospheric forcings. Although the cyclonic nature of basin-scale circulation in the Persian Gulf is well established, the details of the interior circulation remain essentially unknown. To our knowledge, it was only Reynolds (1993) who briefly noted the existence of eddies in the gulf using satellite images. In this paper, we use model results to show that the ICC can deform into a series of mesoscale eddies during late summer and use a variety of observations to verify their existence. The main goal of this work is to show the seasonal evolution of the ICC, its transformation into mesoscale eddies, and their dissipation and to discuss their formation mechanisms briefly. The approach is to use results from a high-resolution (~1 km), regional Hybrid Coordinate Ocean Model (HYCOM) of the Persian Gulf. Model results are complimented by observations of satellite-derived Moderate

Corresponding author address: Prasad Thoppil, Naval Research Laboratory, Code 7323, Stennis Space Center, MS 39529.
E-mail: thoppil@nrlssc.navy.mil

DOI: 10.1175/2010JPO4227.1

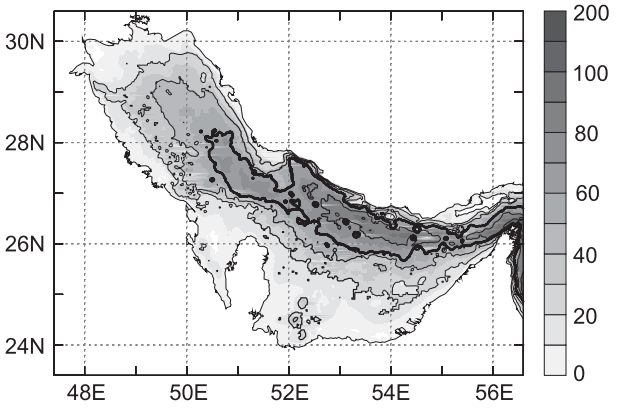

FIG. 1. Model bathymetry in meters. Contours are drawn for 20, 40, 60, 80, and 100 m, with thick lines for 60-m isobaths. The model domain extends northward from 22.3° to 30.7°N and eastward from 47.5° to 59.7°E.

Resolution Imaging Spectroradiometer (MODIS) SST, chlorophyll-*a* concentration, temperature, and salinity from the National Oceanographic Data Center (NODC) and drifter observations.

The outline of the paper is as follows: section 2 introduces the model configuration and forcing fields. Section 3a presents simulated basin-scale circulation and verification using drifter data. The structure of cyclonic circulation with a particular reference to the ICC is presented and validated in section 3b. In section 3c, the transformation of ICC into mesoscale eddies [Iranian coastal eddies (ICE)] as deduced from observations and model is presented. The role of buoyancy-only forcing on the circulation is investigated in a simulation without wind stress forcing in section 3d. Finally, section 4 offers discussion and conclusions of the study.

2. Model description

The HYCOM (Bleck et al. 2002) is used for the ocean circulation simulations. Details of the model configuration and forcing fields are described at length by Thoppil and Hogan (2009) and therefore are only briefly presented here. The model domain extends northward from 22.3° to 30.7°N and eastward from 47.5° to 59.7°E. The model has 16 hybrid vertical layers and horizontal resolution of ~1 km. The baroclinic (barotropic) time step is 60 s (3 s). The eastern boundary is closed (59.7°E) but outfitted with a 50 gridpoint buffer zone (~0.5°) in which temperature, salinity, and pressure are linearly relaxed toward the Generalized Digital Environmental Model version 3.0 (GDEM3) seasonally varying climatological values with an *e*-folding time scale of 1–76 days. GDEM3 is a global gridded ocean temperature and salinity climatology with a horizontal resolution of 1/3° and has 40 vertical levels (Teague et al. 1990; Carnes 2009). The monthly river inflow into the basin is prescribed as precipitation.

The model integration was started from rest on 1 January 2000 using GDEM3 temperature and salinity and integrated for 6 years for the period 2000–05 using 1° 3-hourly U.S. Navy Operational Global Atmospheric Prediction System (NOGAPS) forcing. Furthermore, the model integration is continued for another 5 years (2003–07) using 3-hourly, ½° NOGAPS forcing (which is available only after 2003) in which the winds were corrected for the land–sea contamination (Kara et al. 2007). The results presented here are from the latter run using ½° NOGAPS forcing unless otherwise indicated. From the daily model output for the period 2003–07, a monthly-mean climatology is prepared and presented. In particular, results from the year 2005 are used for detailed analysis of the mesoscale eddy activity.

3. Results

a. Basin-scale circulation

Figure 2 shows depth-averaged velocity vectors in the upper 50 m from the model 5-yr climatology (2003–07) for February, April, June, August, October, and December. The basin-scale circulation pattern simulated by the model agrees with the limited current meter and drifter observations (Reynolds 1993; Abdelrahman and Ahmad 1995) and previous model results (Chao et al. 1992; Blain 2000). In general, the surface current is strongest during the summer (10–20 cm s^{-1}) and weakest (5–10 cm s^{-1}) in the winter. The weaker winter circulation is a result of the reduced density gradient between the Persian Gulf and the Gulf of Oman and because of weak stratification owing to winter cooling. Winter circulation consists of a wind-driven southeastward current (~5 cm s^{-1}) downstream from north of Qatar (Fig. 2a) and density-driven ICC, which flows against the prevailing northwesterly winds.

The current northeast of Qatar maintains its southeastward direction during February, June, and December and becomes weak and varies between southeast and south during other periods (Fig. 2). This current is mostly wind driven; that is, the effect due to density forcing is small because of the very shallow sill depth. Additionally, its existence during winter can be verified using the observations of drifter (M05) trajectory from the Naval Oceanographic Office (NAVO) during the period 4 December 2002–14 April 2003 (Fig. 3a). The drifter gradually moved southeastward between December 2002 and January 2003 at a speed of 4.5 cm s^{-1} and then to the northeast, east of ~54°E (Fig. 3a). The drifter made a recirculation loop in March 2003 and finally drifted toward the coast (54.5°E). The model currents during December 2002 indicate a

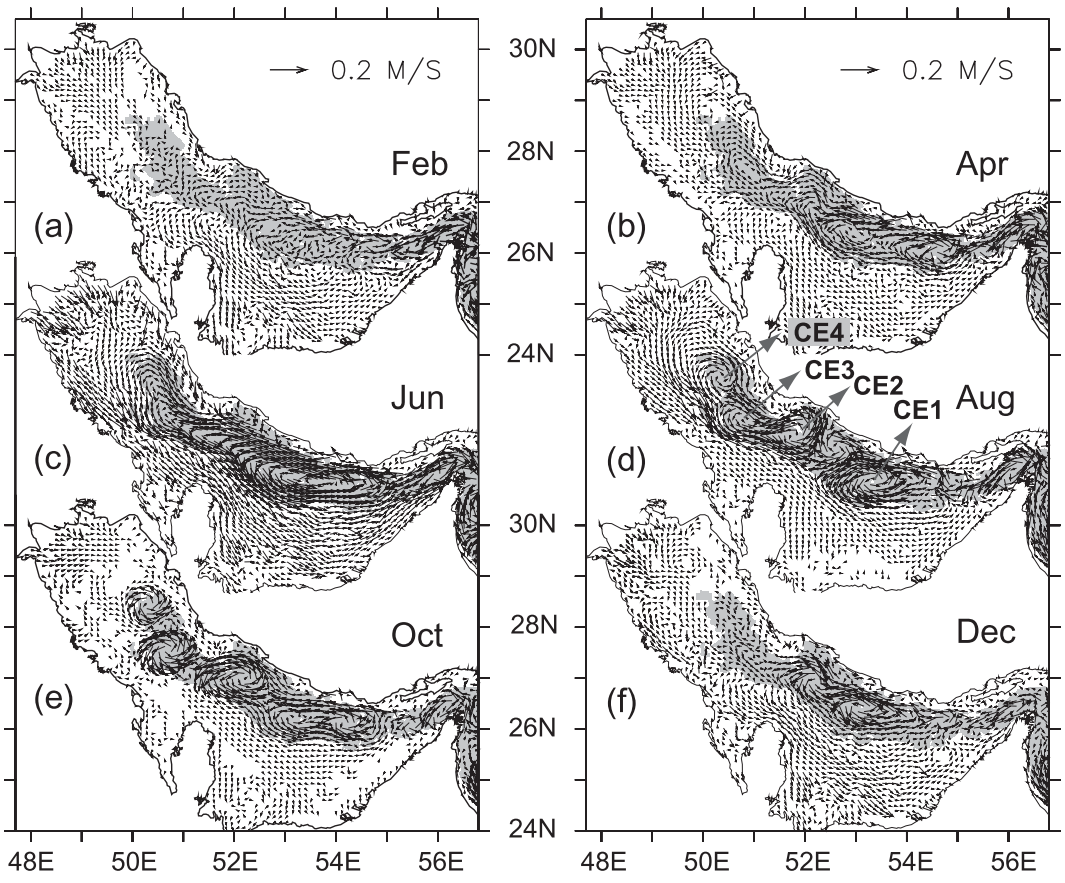

FIG. 2. Monthly-mean currents averaged in the upper 50 m during (a) February, (b) April, (c) June, (d) August, (e) October, and (f) December from the model 5-yr climatology (2003–07). Four cyclonic eddies (CE1, CE2, CE3, and CE4) and the ICC are labeled. For clarity, every 12th vector and current magnitude greater than 5 cm s^{-1} is plotted. Bathymetry deeper than 50 m is shaded in gray.

similar southeastward flow of magnitude ~5 cm s^{-1} (Fig. 3a). It should be noted that the model currents in Fig. 3a are from the simulation that forced with 1° NOGAPS fields. A closer examination of the drifter trajectory during March 2003 revealed a northeastward flow until 3 March 2003, then a southwestward return flow between 3 and 13 March 2003 (Fig. 3b). This short-term flow reversal is evident in the snapshots of model currents between 1 and 7 March (Figs. 3f,b) and is apparently driven by the changes in the wind direction (Fig. 3c).

A cyclonic circulation forms in the central gulf (52°–55°E) during March–April with a northwestward-flowing ICC in its northern flank (Fig. 2b), which veers offshore between 52° and 53°E. Mooring observations of Reynolds (1993) indicated a northwest current at 26.37°N, 53.76°E (M2) and a south and southwest current at 26.84°N, 51.98°E (M4) during March–May 1992 (Fig. 2 of Abdelrahman and Ahmad 1995), characterizing ICC and its offshore branch consistent with the model currents (Fig. 2b). Freshwater discharge from the Shatt-al-Arab combined with northwesterly winds generates a southeastward-flowing current along the coasts of Kuwait and Saudi Arabia during June–September.

Between April and July, the ICC becomes progressively stronger and penetrates far into the northern gulf because of strengthening stratification, increasing inflow, and weakening winds (Fig. 2). The thermocline develops as the ocean gains heat from the atmosphere and generates a strongly stratified water column, which in turn limits the vertical mixing under prevailing weak wind conditions. The pressure gradient generated by the denser (fresher) water residing at the northern (southern) end of the gulf drives freshwater inflow from the Gulf of Oman into the Persian Gulf through the Strait of Hormuz. The northwestward expansion of the freshwater inflow is partly influenced by the diminishing winds, as demonstrated by Chao et al. (1992). The cyclonic circulation in the central gulf (between 52° and 55°E) also widens and intensifies in both its northwest and southeast regions of circulation during June–July, in agreement

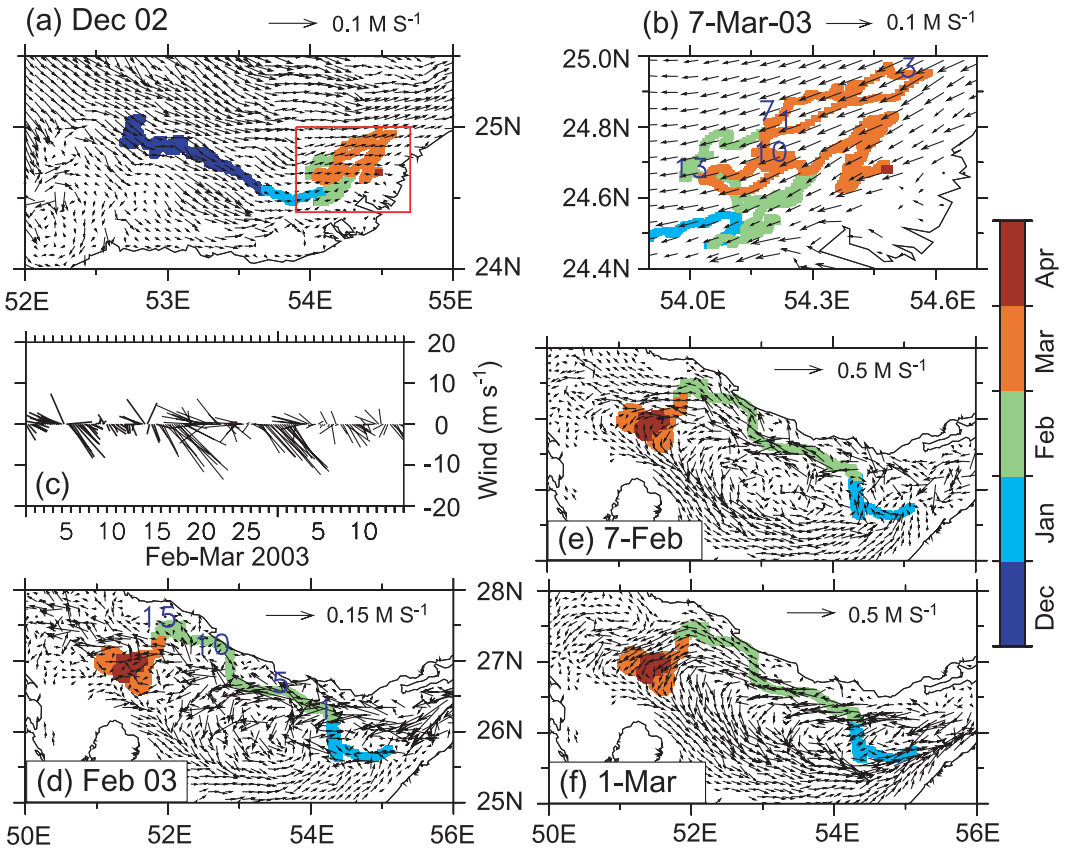

FIG. 3. Comparisons of model currents with the observed drifter trajectories during (a),(b) December 2002 and March 2003 (drifter M5) and (d)–(f) February–March 2003 (drifter M13) and (c) stick plot of Quick Scatterometer (QuikSCAT) wind velocity vectors at 26.5°N, 53°E during February–March 2003. Shading indicates the location and time of the drifters. The drifting period for M5 was 4 Dec 2002–14 Apr 2003 and for M13 it was 22 Jan–14 Apr 2003. Depicted in (b) is the small region shown as red box in (a) during March 2003 indicating a short-term flow reversal. The locations of (b) M5 for 1, 3, 7, 10, and 13 Mar 2003 and (d) M13 for 1, 5, 10, and 15 Feb 2003 are marked. Model currents are shown (a),(b) averaged in the upper 15 m and (d)–(f) at 15 m, an approximate depth of drifters. Shown are (a),(d) monthly-mean currents and (b)–(f) daily snapshots.

with the modeling study of Blain (2000). Mooring observations of Reynolds (1993) during May 1992 also indicated the extension of the flow in M3 and M4 toward the northwest (cf. Figs. 2 and 3 of Abdelrahman and Ahmad 1995).

The cyclonic circulation undergoes significant changes between June and August (Figs. 2c,d), being transformed into a series of mesoscale eddies. Four cyclonic eddies (CE1, CE2, CE3, and CE4) and an anticyclonic eddy (ACE) sandwiched between CE1 and CE2 are evident, which we suggest calling the ICE. They are also evident during October (Fig. 2e) and November (not shown) and their remnants can still be seen in December (Fig. 2f). In sections 3b and 3c, we focus on the two circulation features of interest: 1) evolution of the ICC between February and July and 2) transformation of the ICC into a series of mesoscale eddies during August–September, using model results in conjunction with a variety of observations.

b. ICC

The northwestward-flowing ICC develops in February–March and reaches its maximum strength in June–July (Fig. 2) as the surface inflow through the Strait of Hormuz becomes progressively stronger and with the establishment of the seasonal thermocline. The observed drifter trajectory during January–April 2003 from the NAVO was used to validate the model ICC and its northwestern extent. The drifter (M13) deployed on 22 January 2003 at 25.8°N, 55.1°E, moved along the ICC until 15 February, and drifted south and southwest at about 52°E (Fig. 3d). It made a slight northward turn toward the coast (~26.5°N, 52.8°E) during 7 February and traveled about 260 km between 1 and 15 February 2003 with an average speed of 20 cm s^{-1}. From late February to early March 2003, the drifter moved very slowly south and southwest. Thereafter,

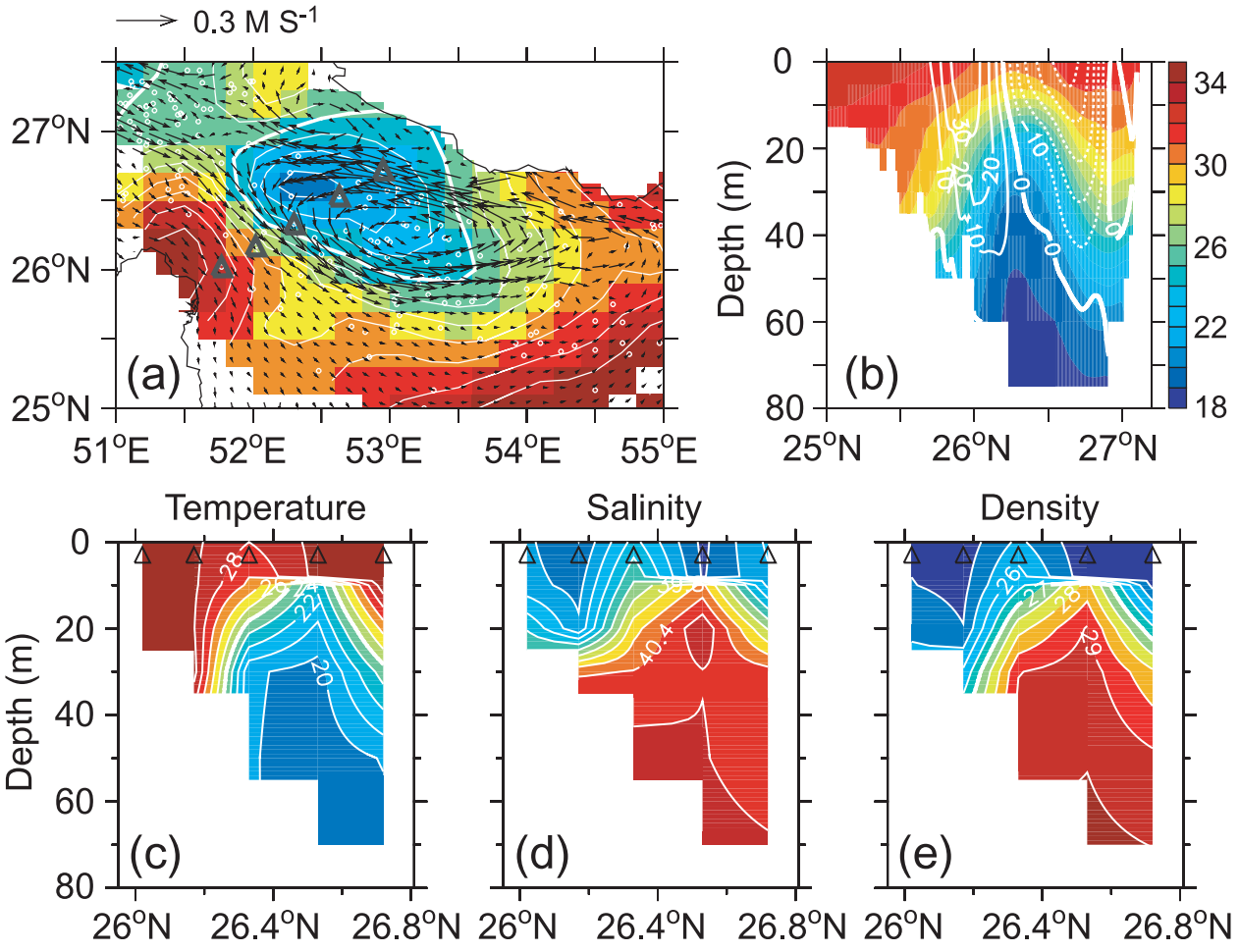

FIG. 4. (a) Horizontally mapped NODC temperature at 30 m (shaded and contoured) with model currents in the upper 50 m during July. Thick contour denotes the 25°C isotherm, and white circles show the NODC data points. (b) Vertical section of temperature (shaded) and zonal velocity (contours, cm s^{-1}) along 53°E during July from the model. Vertical sections of observed (c) temperature, (d) salinity (contour interval is 0.2 psu), and (e) density across the cyclonic circulation [shown as triangles in (a)] during 7 Jul 1968. The packed contours around 10 m indicated a temperature inversion.

the drifter made several closed loops before drifting southeastward.

The simulated ICC is compared with the drifter trajectory qualitatively, whereas detailed Lagrangian analysis will be the focus of a separate study. Model monthly-mean velocity vectors at 15 m (approximate depth of drifters) superimposed on the drifter trajectory for February 2003 are depicted in Fig. 3d. The currents are from the model run that used ½° NOGAPS forcing during the period when the drifter data were collected. The drifter trajectory and the mean velocity vectors show good agreement southeast of 53°E, and they depart between 52° and 53°E during 7–15 February. The model–drifter discrepancy can be associated in part with the short-term changes in the circulation induced by episodic wind events. To probe this further, snapshots of model currents during 7 February and 1 March 2003 are shown in Figs. 3e,f respectively. The ICC, especially its onshore deflection (Fig. 3e) at 52.8°E, and a southwest flow at 52°E (Fig. 3f) are adequately reproduced by the model according to drifter trajectory. The flow intensification during this period is followed by the moderate wind events of 8–10 m s^{-1} (Fig. 3c). The drifter closely followed a trajectory along 50–60-m isobaths, and it veered offshore at 27.5°N, 52°E, where the continental shelf becomes wider and shallower (Fig. 1). In addition to the shallower and wider shelf, there is an opposing weak southeastward coastal flow along the Iranian coast in the northern gulf (Figs. 2a, 3f) that might have contributed to the offshore turning of the current.

The cyclonic circulation in the central gulf (52°–55°E) becomes progressively stronger between April (Fig. 2b) and July (Fig. 4a). The vertical section of zonal velocity along 53°E during July (Fig. 4b) indicated a maximum

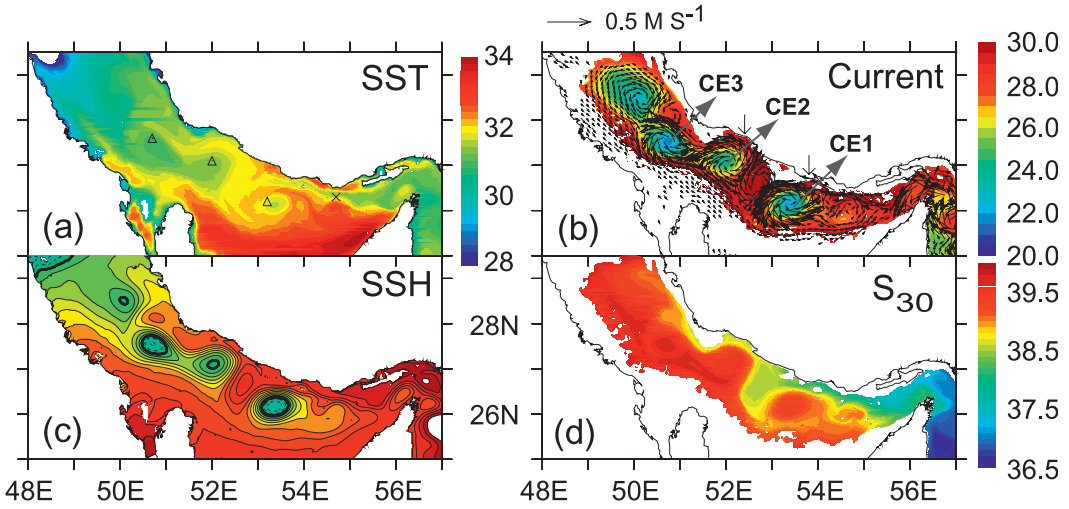

FIG. 5. Model (a) SST, (b) temperature at 30 m with overlaid velocity vectors in the upper 30 m, (c) SSH (contour interval is 0.01 m; thick line for zero contour), and (d) salinity at 30 m during September 2005. Dark arrows in (b) show the locations where the ICC separate from the coast. Three cyclonic eddies, CE1 (26.2°N, 53.2°E), CE2 (27.1°N, 52°E), and CE3 (27.6°N, 50.7°E), are marked with triangles and a cusp-shaped SST feature (26.3°N, 54.7°E) with an x in (a).

velocity of 40 cm s^{-1} along the ICC, which is twice the magnitude it was in February, accompanied by weaker counter flow (~5 cm s^{-1}) at depths. On the southern side, a returning eastward current (30 cm s^{-1}) occurs. The NODC temperature at 30 m (which is objectively mapped) shown in Fig. 4a for July supports the existence of a cyclonic circulation similar to that depicted in the model. The closed contours of temperature less than ~25°C characterize a thermal dome associated with the cyclonic cell. To illustrate this further, vertical sections of temperature, salinity, and density along a section across the cyclonic cell during 7 July 1968 from the NODC are displayed in Figs. 4c,d,e, respectively. The doming of isotherms and associated sloping isopycnals reflect a cyclonic circulation. The 24°C isotherm in the observation was raised by 20 m (Fig. 4c), which is compatible with that in the model (Fig. 4b). The sloping isopycnals downward on either side of the coasts manifests alongshore flows. The relatively low-salinity water in the upper 20 m (38.8 psu) by the Iranian coast and the region south of 26.2°N suggests that it is carried by the ICC from the Gulf of Oman and then transported to the south by the ICC veering onto the southern shelf.

c. *ICE*

An intriguing aspect of circulation in the Persian Gulf is the deformation of the ICC into several energetic mesoscale eddies during August (ICE; Fig. 2d). We chose the year 2005 as a typical period to elucidate their evolution. Other years also showed similar eddies, but they are not presented. As in the August climatology (Fig. 2d), eddies are apparent in the model temperature, salinity, currents, and sea surface height (SSH) during September 2005 (Fig. 5). The shape of eddies range from circular to somewhat elliptical. The eddies have a strong signature in the temperature at 30 m and currents (Fig. 5b) and a weaker signature in the SST (Fig. 5a). The coastal current veers offshore at two locations: ~26.6°N, 53.8°E and 27.5°N, 52.4°E (indicated by black arrows in Fig. 5b), generating two cyclonic eddies CE1 and CE2 with diameters ranging from 130 to 119 km. CE1 has a peak zonal velocity of 40 (30) cm s^{-1} at the northern (southern) side. There is a weak anticyclonic eddy sandwiched between CE1 and CE2 seen in the SSH and currents. Figure 5b also shows two more cyclonic eddies (CE3 and CE4). The CE4 (~28.5°N, 50.5°E) is much weaker than the other eddies because of the shallower bathymetry (50–60 m; Fig. 1). The cyclonic eddies have colder (~23°C) and saltier (~39.5 psu) water in their core. The CE1 displaced the depth of the 24°C isotherm by 25 m. With salinity increasing downward, cyclonic eddies bring saltier water from below and form high-salinity cores.

Satellite images are used to confirm the existence of the eddies. They are mostly cloudy, but a clear image of MODIS-derived chlorophyll-*a* concentration during 17 September 2005 showed a series of eddies (Fig. 6a). A superimposition of model currents on the chlorophyll-*a* map (Fig. 6b) for the same period clearly demonstrates that the locations of the eddies are in very good agreement with those in the model (CE1, CE2, and CE3). The evidence for a fourth cyclonic eddy CE4 was missing in the chlorophyll image during 17 September 2005. However,

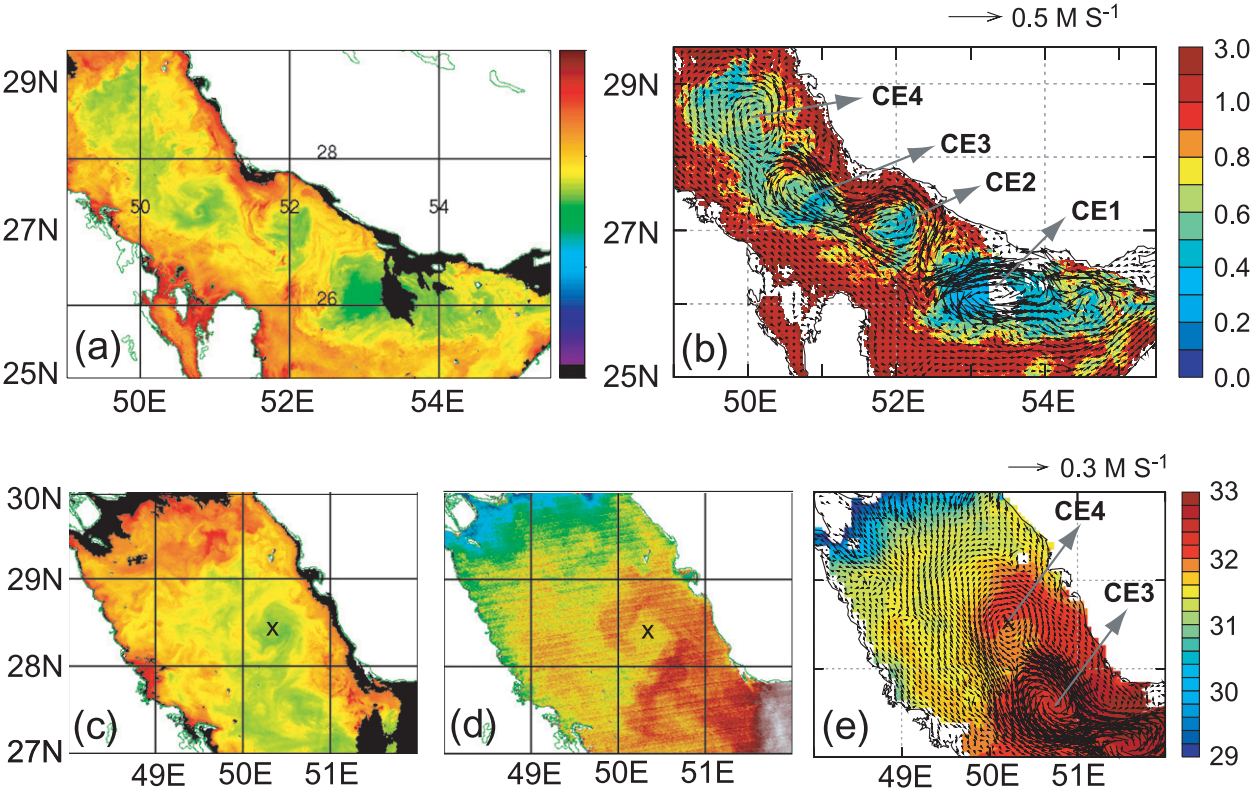

FIG. 6. (a) MODIS-derived (1 km) chlorophyll-*a* concentration (mg m^{-3}) and (b) model currents in the upper 50 m during 17 Sep 2005 overlaid on the chlorophyll-*a* map. MODIS 1-km (c) chlorophyll-*a*, (d) SST during 21 Sep 2003, (e) model currents in the upper 30 m overlaid on the MODIS 4-km SST during September 2003. Ocean color provides a better depiction of four cyclonic eddies (CE1, CE2, CE3, and CE4), and their locations compare quite well with that in the model. The center of CE4 is marked with an x. It is suffice to mention that green color represents lower concentrations and yellow and red colors represent high concentrations, because we are not concerned with the magnitude of the chlorophyll concentrations.

the chlorophyll-*a* and SST during 21 September 2003 revealed the CE4 (Figs. 6c,d) in accordance with that in the model for the same period (Fig. 6e). The eddies have low chlorophyll-*a* (<1 mg m^{-3}) in the core and elevated chlorophyll-*a* (>1 mg m^{-3}) in their periphery. The eddies transport high chlorophyll, nutrient-rich coastal waters offshore thereby generating regions of enhanced chlorophyll-*a* between the eddies. Thus, the model is successful in reproducing the observed characteristics of the eddies: their size, shape, locations, and time of occurrence.

The temporal evolution of ICE illustrated in weekly maps of MODIS 4-km SST from 29 August to 22 September 2005 (Fig. 7) suggests that the eddies appear rather quickly. The eddies began to appear during 6 September, mature by 14 September, and become less discernable during 22 September. The SST during 29 August exceeds 33°C everywhere except in the vicinity of Strait of Hormuz (east of 54°E), where relatively colder SSTs (<32°C) occur. The northwestward progression of this cold water along the Iranian coast by 6 September (Fig. 7b) demarcates the first cyclonic eddy (CE1). At this time CE2 makes its appearance northwest of CE1, with relatively warmer water in the periphery. Fully developed eddies (CE1, CE2, and CE3) are evident during 14 September 2005, and their centers, indicated by triangles, coincide with that in the model (Fig. 5a).

The appearance of eddies coincident with the progression of cold water along the Iranian coast can be explained in light of the two moderate wind events (~8–10 m s^{-1}) that occurred during 5 and 14 September 2005 (Fig. 7e). These events produced increasing inflow through the Strait of Hormuz; as a result, the relatively cold water from the Strait of Hormuz advected northwestward along the Iranian coast. This, combined with wind-driven vertical mixing, yielded clear signatures of eddies in the SST maps. The first wind event also caused SST cooling of 1°–2°C in the northwestern region west of 51°E between 29 August and 6 September 2005 (Figs. 7a,b). To quantify the SST cooling mechanisms, we examined daily values of net heat flux and SST from the objectively analyzed air–sea fluxes (OAFlux; Yu and Weller 2007). In response to the

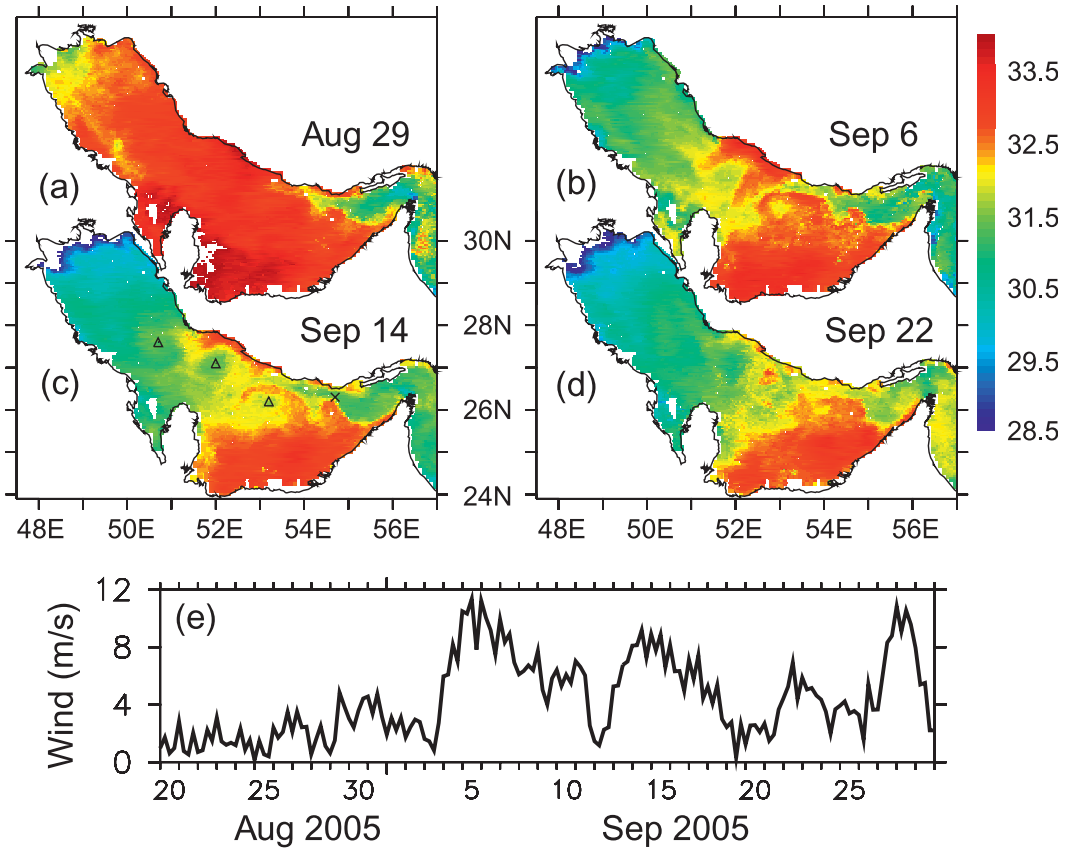

FIG. 7. MODIS-derived (4 km) weekly maps of SST during (a) 29 Aug, (b) 6 Sep, (c) 14 Sep, and (d) 22 Sep 2005 depicting the temporal evolution of the ICE and (e) 6-hourly cross-calibrated multiplatform (CCMP) wind speed (Atlas et al. 2009) at 27°N, 51°E during 20 Aug–30 Sep 2005 showing two moderate wind events. Three cyclonic eddies and their centers, CE1 (26.2°N, 53.2°E), CE2 (27.1°N, 52°E), and CE3 (27.6°N, 50.7°E), are labeled with triangles, and x denotes a cusp-shaped SST feature (26.3°N, 54.7°E) during 14 Sep 2005.

first wind event, the northwestern gulf experienced a net heat loss of 200–300 W m^{-2}. A simple one-dimensional heat balance calculation suggests that the surface heat loss is responsible for the SST cooling by 1°–2°C, assuming a mixed layer depth of 15 m. However, the impact of second wind event on the SST cooling is negligibly small.

Eddies are often identified by means of SST images because an eddy typically has a different temperature than its surroundings. However, the spatially uniform cap of warm water over the gulf during 29 August 2005 (Fig. 7a) under weak wind conditions may have masked the signature of eddies. To investigate whether the eddies were present on or before 29 August 2005 and to show their temporal evolution, we employ sequences of model currents during the July–August 2005 period for days 6, 12, 18, 24, and 30 of each month (Fig. 8). It is clear that the eddies are present in the model currents even before they were first detected in the MODIS SST (Fig. 7b). The cyclonic circulation seen in the central gulf (52°–55°E) during early July transforms into a series of eddies by late July. The first eddy develops from the meandering ICC ($u_{z=0}$ = 80 cm s^{-1}) between 6 and 18 July. During this period, the western terminus of ICC retreats from ~51.5° to ~52.5°E and the strengthening of an anticyclonic eddy at the northwestern corner appears to constrain its westward expansion. The circulation during 24 July consists of a cyclonic and an anticyclonic eddy (described as a dipole eddy pair). Over the next few days, the cyclonic eddy gains strength while its counterpart loses its identity. By 12 August, the cyclonic eddy becomes elliptical and remains near stationary while its major axis rotates in a counterclockwise direction. As the angle between the major axis and Iranian coast increases, the anticyclonic eddy reappears and intensifies northwest of the cyclonic eddy. The size of this eddy is similar to its counterpart on 30 August. There are two more cyclonic eddies that begin to form in late July whose intensity grows with time (20–30 cm s^{-1}) while remaining stationary. By 30 August, there are a total of five eddies: three cyclonic eddies and two ACE, although some are transient. As expected, they are

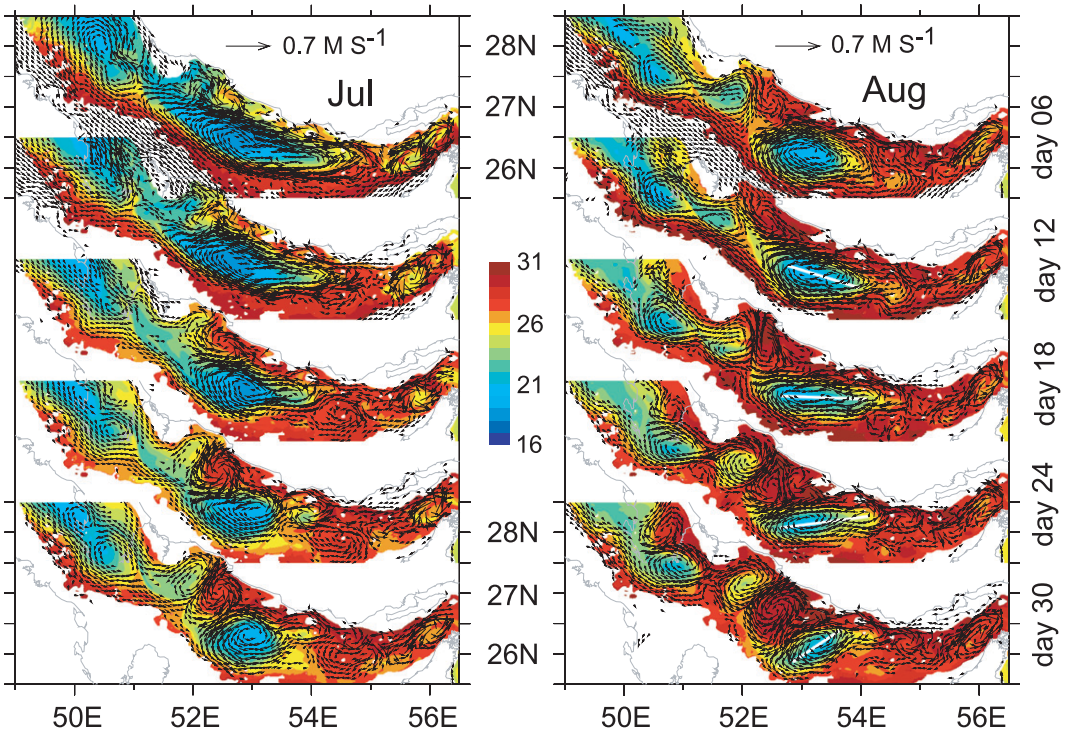

FIG. 8. Daily snapshots of model velocity vectors (m s^{-1}) in the upper 50 m overlaid on the temperature at 30 m during July–August 2005 for days 6, 12, 18, 24, and 30, illustrating the transformation of the ICC into a series of both cyclonic and anticyclonic eddies (ICE). The white lines indicate the orientation of CE1. For clarity, velocity vectors larger than 4 cm s^{-1} are plotted.

characterized as cold (cyclonic) and warm (anticyclonic) core eddies (Fig. 8).

d. Role of wind stress forcing

It has been shown that the ICC is the strongest current in the gulf whose strength is related to the inflow–outflow through the Strait of Hormuz, strong stratification, and decreasing winds. To discern the role of wind stress forcing and the associated Ekman drift on the ICC and the generation of ICE, we performed a model experiment without wind stress forcing ($\tau_x = \tau_y = 0$) from January to December 2005 while keeping the wind speed unchanged. The resulting flow is primarily buoyancy driven. A comparison of this run with the control run reveals that wind stress forcing does have a major impact on the overall circulation pattern (Fig. 9). The ICC is strong (40 cm s^{-1}) in the control run in June 2005 (Fig. 9a) and the MODIS SST corroborates its core as a narrow band of relatively warm water by the Iranian coast slightly offshore (inset plot). The simulation did reproduce the ICC; however, it is weaker (reduced from 40 to 25 cm s^{-1}) and narrower than the control run (Fig. 9b), suggesting the important role of Ekman drift resulting from the prevailing northwesterly winds. The ICC can also be influenced remotely by the fluctuations in wind stress via forcing a variable surface inflow through the Strait of Hormuz. A notable difference in the circulation is the weakening of the southeastward current south of the ICC (reduced from 20 to 5 cm s^{-1}) primarily because of the absence of northwesterly wind stress.

The changes in the cross-shelf density structure induced by wind stress along 53°E is depicted in Fig. 10. In the control run, the isopycnals tilt downward on either side of the coasts, implying strong alongshore flows (Fig. 10a) that in turn are maintained through geostrophy. This density pattern agrees qualitatively well with the early July observations shown in Fig. 4e. A partial relaxation of the cross-shelf density gradient (sloping isopycnals) in the absence of Ekman dynamics signifies a weaker ICC. On the southern side, the isopycnals in the buoyancy-only forcing case are almost flat near the surface, indicating a weak flow (5 cm s^{-1}). The downward tilt of isopycnals toward the coast below ~30 m suggests an eastward current near the bottom apparently resulting from the sinking and spreading of saltier water.

The mesoscale eddies (ICE) generated by the buoyancy-only forcing experiment during September 2005 are consistent with the buoyancy plus Ekman drift forcing

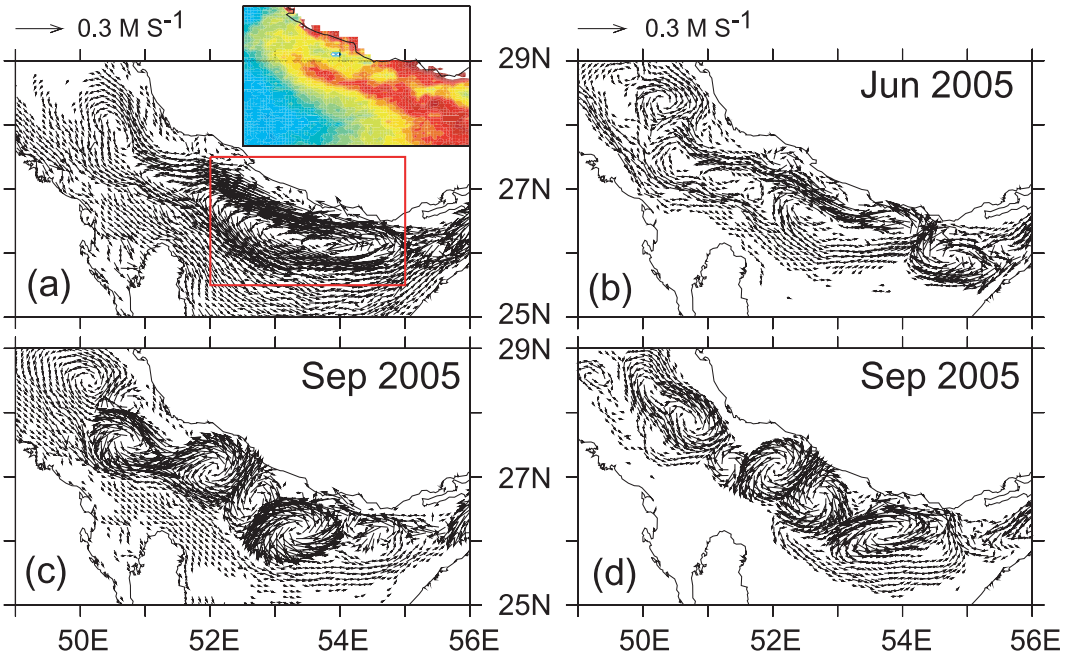

FIG. 9. Model currents in the upper 50 m during June and September 2005 from the simulations (a) with (control run) and (b) without wind stress forcing. In the case with no wind stress forcing, neither the wind speed nor the buoyancy forcing (air–sea heat fluxes and evaporation) is unchanged from the control run. The inset shows the MODIS SST during June 2005 for the region shown in red box corroborating the model ICC. For clarity, velocity vectors larger than 2 cm s^{-1} are plotted.

(Figs. 9c,d). The transformation of the ICC into ICE takes place despite the differences in circulation during June 2005 (Figs. 9a,b). The significant weakening of a southeastward current south of ICC during June appears less important in the meandering and eddies-generating processes. The eddies have similar characteristics, except that 1) their centers are displaced slightly to the east, 2) a cyclonic eddy (CE1) is weaker and an anticyclonic eddy (between CE1 and CE2) is stronger, and 3) the eddies CE2 and CE3 are detached (Fig. 9d). These changes are primarily the result of the stratification being modulated by the wind-driven mixing and Ekman drift. The model sensitivity experiment suggests that the eddies evolve from the ICC as it becomes progressively stronger and unstable.

4. Discussion and conclusions

The seasonal variability of circulation and mesoscale eddies in the Persian Gulf are studied using the results from an ~1 km Hybrid Coordinate Ocean Model (HYCOM), forced by ½° NOGAPS atmospheric data. The relative role of buoyancy versus Ekman dynamics on the circulation is investigated in a perturbation experiment without wind stress forcing while keeping the wind speed unchanged. The basin-scale circulation and eddies simulated by the model are validated using the drifter trajectory, NODC observations, and satellite images. The simulation, in particular, reproduced the observed characteristics of the eddies quite well.

A quasi-permanent cyclonic circulation develops in the central gulf (52°–55°E) during March–April, and it progressively expands northwestward until July, which is in agreement with the summary by Reynolds (1993). The northwestward-flowing Iranian Coastal Current (ICC) from the Strait of Hormuz to north of Qatar (52°E) forms the northern flank of the circulation. This is the strongest current in the gulf, reaching its peak strength in July with a magnitude exceeding 40 cm s^{-1}, accompanied by weaker counter flow (~5 cm s^{-1}) at depths. The cross-shelf density structure across the ICC indicates isopycnals sloping downward toward the north implying a strong alongshore current. The resulting cross-shelf pressure gradient in turn maintains an alongshore current through geostrophy. The ICC becomes weaker and narrower in the buoyancy-only forcing experiment. A southeastward current demarcates the southern branch of the cyclonic circulation with a small part exiting through the Strait of Hormuz. The significant weakening of this current in the buoyancy-only forcing experiment demonstrates that this flow is associated with the Ekman drift driven by the prevailing northwesterly winds. Thus, both Ekman dynamics and buoyancy identify as the two processes contributing to the maintenance of a cyclonic circulation.

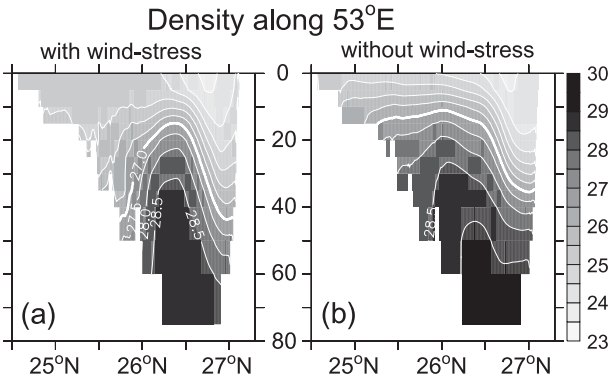

FIG. 10. Vertical section of density (contour interval is 0.5) along 53°E during June 2005 from the simulations (a) with (control run) and (b) without wind stress forcing. The isopycnals slope downward toward the Iranian coast.

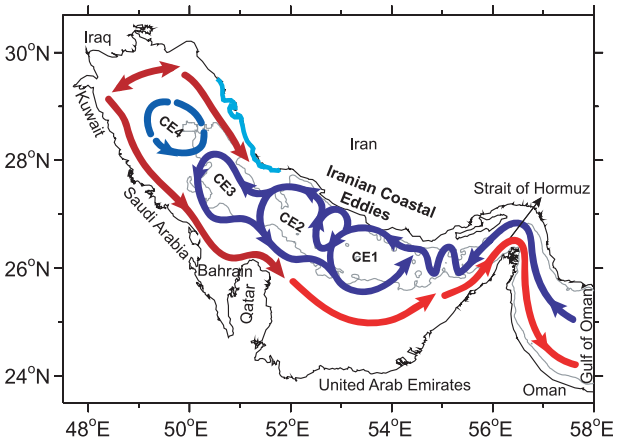

FIG. 11. Schematic diagram showing circulation in the Persian Gulf. The northwestward-flowing ICC becomes unstable as a result of baroclinic instability and evolves into a series of mesoscale cyclonic eddies (CE1, CE2, CE3, and CE4), which we call the ICE, during August–September. The 50-m isobaths are shown in gray color. Blue color arrows indicate the inflow of low-salinity water from the Gulf of Oman, and red color arrows indicate the outflow of high-salinity Persian Gulf Water (PGW). Blue shades along the Iranian coast indicate upwelling.

The cyclonic circulation undergoes significant changes between July and August by transforming into three to four cyclonic eddies (CE1, CE2, CE3, and CE4; Fig. 3) and often an anticyclonic eddy (ACE) sandwiched between CE1 and CE2. The presence of these eddies, which we collectively denote as the Iranian coastal eddies (ICE), dominate the circulation over a relatively larger area during August–October. The eddies have a diameter of about 115–130 km and vertically extend over most of the water column. They remain stationary at the same location, while undergoing some distortions by merging or disengaging two eddies during their life cycle. The remnants of eddies are seen until November, and they dissipate thereafter as the winter cooling causes the thermocline to collapse. The characteristics of eddies in terms of their size and shape produced by the model agree quite well with that deduced from the MODIS SST and chlorophyll observations. These eddies recur every year during the period analyzed here (2003–07); however, their characteristics show considerable interannual variability (not shown).

Although the discussion of the mechanisms behind the origin of the eddy field is beyond the scope of this paper, the sequence of events leading to the transformation of the ICC into eddies can be summarized as follows: First, the northwestward-flowing ICC becomes progressively stronger and unstable between July and August because of an instability mechanism (Fig. 9). Second, the meanders grow in the ICC, and they contain the southeastward current south of the ICC. Finally, the eddies evolve from turbulent cascades and feedbacks processes that require an energy source. If the source of energy for the instability is large, the eddies are active enough so that the nonlinear interactions continue until the turbulent cascade occurs. Thus, the initial scale of growth changes to other scales. A possible energy source is the potential energy stored in the isopycnal tilt (Fig. 10a), which can be released through baroclinic instability. Thus, the mechanism behind the turbulent cascade is baroclinic instability. These two processes do not necessarily conflict with each other. The relaxation of warmer and fresher water inflow through the Strait of Hormuz in late July could generate a perturbation in the cross-shelf density field and trigger the baroclinic instability process. It is worth mentioning that the progression of a salinity front that separates the low-salinity water from the Gulf of Oman and high-salinity water in the Persian Gulf is accompanied by the development of eddies. Considering the baroclinic Rossby deformation radius of ~25–30 km and a typical eddy size of ~110 km, the generation of the eddies is consistent with the baroclinic instability process. However, further study is needed to identify and quantify the nature of the instability, including kinetic and potential energy budgets by employing models that vary from simple to complex. This is one area where we set forth avenues for future research.

On the basis of the model results and model–data comparisons, we have for the first time demonstrated the development of a series of mesoscale eddies and constructed a new schematic of the general circulation in the Persian Gulf for the period between August and November (Fig. 11). The typical basin-scale circulation pattern during the remaining period is cyclonic in spite of its strong seasonal variability as demonstrated by Reynolds (1993) and this study. Additional observational

programs in conjunction with numerical modeling would aid in our understanding of the complex circulation that is unraveled in this study. The recurring eddies in the Persian Gulf, in a broader sense, resemble those in other closed or semienclosed basins (e.g., Mediterranean Sea, Black Sea, Adriatic Sea, Gulf of California).

Although the simulation reproduced many of the observed circulation features, especially the previously unknown mesoscale eddies, the model has several shortcomings that need to be addressed in future studies. First, tidal forcing has not been included, but efforts are underway. However, Blain (1998, 2000) and Azam et al. (2006) confirmed that the tidal influence on the overall circulation in the Persian Gulf is minimal (less than 2 cm s^{-1}), except in a few localized areas (e.g., the Iranian coast and the Strait of Hormuz) where the tidal residuals are large enough to enhance the dominant density-driven flow. Second, although simulated salinity qualitatively agrees with the observations, the dense water formation events are not well depicted as is to be expected because of damping of sea surface salinity (SSS) to climatology. A short test run (1 yr) without salinity relaxation did produce a salinity of ~42 psu during winter, which compares very favorably with the observations. Finally, the model's eastern boundary (60°E) is relaxed to the seasonal climatology of temperature, salinity, and pressure. Although this approach has been widely used for Persian Gulf modeling, we did a test run using the boundary conditions extracted from a $^1/_{12}°$ global HYCOM. Preliminary analysis suggests no visible changes in the overall circulation within the Persian Gulf. Nevertheless, the major conclusions drawn in this study remain valid even if we had addressed the above model shortcomings.

Acknowledgments. This paper is a contribution to the coastal ocean nesting studies project sponsored by the Office of Naval Research (ONR) under Program Element 601153N. It is also a contribution to the NRL project Full Column Mixing for Numerical Ocean Models. The simulations were performed on IBM-SP4 workstations at the Naval Oceanographic Office under a grant of computer time from the DoD High Performance Computer Modernization Office (HPCMO). Alan Wallcraft is thanked for his substantial contribution to this effort through his work on model development and his computer expertise. The insightful comments from the two reviewers helped improve the quality of the paper, and we thank them for their thorough review. We are extremely grateful to Dr. Frank Bub for drifter data from the Naval Oceanographic Office (NAVO). We have benefited from discussions with M. Ikeda, Hokkaido University, and J. Richman, NRL. MODIS data (available online at http://poet.jpl.nasa.gov and http://oceancolor.gsfc.nasa.gov) and NODC data (available online at http://www.nodc.noaa.gov) were downloaded.

REFERENCES

Abdelrahman, S. M., and F. A. Ahmad, 1995: Note on the residual currents in the Arabian Gulf. *Cont. Shelf Res.,* **15,** 1015–1022.

Atlas, R., R. N. Hoffman, J. Ardizzone, S. M. Leidner, and J. C. Jusem, 2009: Development of a new cross-calibrated, multi-platform (CCMP) ocean surface wind product. Preprints, *13th Conf. on Integrated Observing and Assimilation Systems for Atmosphere, Oceans, and Land Surface (IOAS-AOLS),* Phoenix, AZ, Amer. Meteor. Soc., 4B.1. [Available online at http://ams.confex.com/ams/pdfpapers/145957.pdf.]

Azam, M. H., W. Elshorbagy, T. Ichikawa, T. Terasawa, and K. Taguchi, 2006: 3D model application to study residual flow in the Arabian Gulf. *J. Waterw. Port Coastal Ocean Eng.,* **132,** 1–13.

Blain, C. A., 1998: Barotropic and tidal residual circulation in the Arabian Gulf. *Proc. Fifth Int. Conf. on Estuarine and Coastal Modeling,* Alexandria, VA, American Society of Civil Engineers, 166–180.

——, 2000: Modeling three-dimensional thermohaline-driven circulation in the Arabian Gulf. *Proc. Sixth Int. Conf. on Estuarine and Coastal Modeling,* Reston, VA, American Society of Civil Engineers, 74–93.

Bleck, R., G. R. Halliwell, A. J. Wallcraft, S. Carroll, K. Kelly, and K. Rushing, 2002: HYbrid Coordinate Ocean Model (HYCOM) user's manual: Details of the numerical code. HYCOM, 177 pp. [Available online at http://www.hycom.org/attachments/063_hycom_users_manual.pdf.]

Carnes, M. R., 2009: Description and evaluation of GDEM-V3.0. NRL Rep. NRL/MR/7330–09-9165, 24 pp.

Chao, S.-Y., T. W. Kao, and K. R. Al-Hajri, 1992: A numerical investigation of circulation in the Arabian Gulf. *J. Geophys. Res.,* **97,** 11 219–11 236.

Elshorbagy, W., M. H. Azam, and K. Taguchi, 2006: Hydrodynamic characterization and modeling of the Arabian Gulf. *J. Waterw. Port Coastal Ocean Eng.,* **132,** 1–10.

Horton, C., M. Clifford, D. Cole, J. Schmitz, and L. Kantha, 1992: Operational modeling: Semienclosed basin modeling at the Naval Oceanographic Office. *Oceanography,* **5,** 69–72.

Hunter, J. R., 1983: Aspects of the dynamics of the residual circulation of the Arabian Gulf. *Coastal Oceanography,* H. G. Gade, A. Edwards, and H. Svendsen, Eds., Plenum, 31–42.

Kämpf, J., and M. Sadrinasab, 2006: The circulation of the Persian Gulf: A numerical study. *Ocean Sci.,* **2,** 1–15.

Kara, A. B., A. J. Wallcraft, and H. E. Hurlburt, 2007: A correction for land contamination of atmospheric variables near land–sea boundaries. *J. Phys. Oceanogr.,* **37,** 803–818.

Lardner, R. W., and S. K. Das, 1991: On the computation of flows driven by density gradient: Residual currents in the Arabian Gulf. *Appl. Math. Model.,* **15,** 282–294.

——, W. J. Lehr, R. J. Fraga, and M. A. Sarhan, 1987: Residual currents in the Arabian Gulf I: Density driven flow. *Arabian J. Sci. Eng.,* **12,** 341–354.

——, ——, ——, and ——, 1988: A model of residual currents and pollutant transport in the Arabian Gulf. *Appl. Math. Model.,* **12,** 379–390.

——, A. H. Al-Rabeh, N. Gunay, and H. M. Cekirge, 1989: Implementation of the three-dimensional hydrodynamic model for the Arabian Gulf. *Adv. Water Res.,* **12,** 2–8.

——, ——, ——, H. Hossain, R. M. Reynolds, and W. J. Lehr, 1993: Computation of the residual flow in the Gulf using the *Mt*

Mitchell data and the KFUPM/RI hydrodynamical models. *Mar. Pollut. Bull.,* **27,** 61–70.

Reynolds, R. M., 1993: Physical oceanography of the Gulf, Strait of Hormuz and the Gulf of Oman—Results from the *Mt. Mitchell* expedition. *Mar. Pollut. Bull.,* **27,** 35–59.

Song, Y., S. K. Das, and R. W. Lardner, 1994: Computation of density driven flows using the spectral method: Application to the Arabian Gulf. *Cont. Shelf Res.,* **14,** 1039–1052.

Teague, W. J., M. J. Carron, and P. J. Hogan, 1990: A comparison between the Generalized Digital Environmental Model and Levitus climatologies. *J. Geophys. Res.,* **95,** 7167–7183.

Thoppil, P. G., and P. J. Hogan, 2009: On the mechanisms of episodic salinity outflow events in the Strait of Hormuz. *J. Phys. Oceanogr.,* **39,** 1340–1360.

Yu, L., and R. A. Weller, 2007: Objectively analyzed air–sea heat fluxes for the global ice-free oceans (1981–2005). *Bull. Amer. Meteor. Soc.,* **88,** 527–539.